Plant growth simulation for landscape-scale hydrological modelling

J. R. KINIRY[1], J. D. MACDONALD[2], ARMEN R. KEMANIAN[3], BRETT WATSON[4], GORDON PUTZ[4] & ELLIE E. PREPAS[5]

1 *US Department of Agriculture, Agricultural Research Service, 808 E. Blackland Road, Temple, Texas 76502, USA*
  jim.kiniry@ars.usda.gov

2 *Agriculture et Agroalimentaire Canada, Québec G1V 2J3, Canada*

3 *Blackland Research and Extension Center, Texas AgriLife Research, 720 E. Blackland Road, Temple, Texas 76502, USA*

4 *Department of Civil and Geological Engineering, University of Saskatchewan, 57 Campus Drive, Saskatoon, Seskatchewan S7N 5A9, Canada*

5 *Department of Forestry and the Forest Environment, Lakehead University, 955 Oliver Road, Thunder Bay, Ontario P7B 5E1, Canada*

Abstract Landscape-scale hydrological models can be improved by incorporating realistic, process-oriented plant models for simulating crops, perennial grasses and woody species. The objective of this project was to present some approaches for plant modelling applicable to daily time step hydrological transport models, such as SWAT. Accurate simulation of plant growth can improve the accuracy of simulations of hydrological and biogeochemical cycles. First, we describe some unique aspects of the general plant model ALMANAC. Next, we describe a modification of the original ALMANAC model used to simulate complex successional vegetation changes in the years following disturbance of a variety of different forest eco-systems, such as forest fires, clear cuts and insect infestations. Finally, we discuss alternative physiological and physical process simulation techniques of plant growth that could increase simulation accuracy in landscape-scale hydrological and transport models such as SWAT.

Key words Beer's law; forestry modelling; leaf area index; plant simulation; radiation use efficiency

Simulation de croissance végétale au service de la modélisation hydrologique a l'échelle du paysage

Résumé Les modèles hydrologiques qui fonctionnent à l'échelle du paysage peuvent être améliorés en incorporant des modèles de plante réalistes orientés sur les processus pour simuler les cultures, les prairies permanentes et les espèces ligneuses. Ce projet a eu pour but de présenter quelques approches de modélisation des plantes intégrables au sein de modèles hydrologiques à pas de temps journalier, comme le modèle SWAT. Une simulation précise de la croissance végétale peut améliorer la précision des simulations des cycles hydrologiques et biogéochimiques. Nous commençons en décrivant quelques aspects originaux du modèle végétal général ALMANAC. Puis nous décrivons une modification de la version originale d'ALMANAC pour simuler des changements complexes de succession végétale au cours des années qui suivent la perturbation d'un écosystème forestier, comme un incendie de forêt, une coupe claire ou une infestation d'insecte. Finalement, nous discutons quelques techniques alternatives pour simuler les processus physiologiques et physiques de la croissance végétale qui pourraient améliorer la précision des simulations de végétation dans les modèles hydrologiques à l'échelle du paysage comme SWAT.

Mots clefs loi de Beer; modélisation forestière; indice de surface foliaire; simulation de plante; efficacité de l'utilisation du rayonnement

INTRODUCTION

Realistic, process-oriented plant models that can easily simulate different crops, grasses, and woody species are valuable for landscape-scale hydrological transport models. Comprehensive hydrological models integrate information from a wide range of sources into easily-applied decision aids useful for agricultural producers, crop consultants, and policy makers. Currently, plant growth in SWAT assumes a uniform, single plant species community. Thus dynamic plant mixtures such as trees and grasses or temporal changes in species composition cannot be simulated by the model in its present form. Incorporating accurate plant simulation into hydrological models can improve such decision aids. Our goal was to present different approaches for plant modelling applicable to daily time step hydrological transport models such as SWAT (Soil Water Assessment Tool) (Arnold *et al.*, 1998) that can affect simulation accuracy for several components of water and nutrient biogeochemical cycles.

Robust models for crops, grasses, and trees provide quantitative means to predict hydrological consequences of various management decisions under different environmental and climatic conditions. These include harvesting schemes, replanting, fertilizer applications, and control of undesirable plants. Management decisions for annual crops or perennial pastures typically consider spatial and temporal scales different from that of forest management. In crop and pasture management, the spatial focus ranges from single fields to whole farms and small watersheds. In contrast, foresters' objectives focus on long-term management of large sectors of forests. Large-scale hydrological modelling helps to minimize local disturbance due to tree harvests (on the scale of first order watersheds) and to avoid long-term cumulative impacts on a larger scale (third and fourth order watersheds) of both water quantity and water quality. Thus, balancing the representation of such diverse vegetative covers in comprehensive models like SWAT requires careful consideration of the objectives and level of detail required to achieve desired accuracy in simulating water fluxes and water quality.

As simulation problems become more complex, there may be a need for more complex representation of vegetation processes. Field-scale models such as those in SWAT and ALMANAC provide a general description of the growth of a vegetative canopy using deterministic relationships based on physiological or physical processes. Leaf growth is often represented by the leaf area index (LAI). Yield can be simulated using a harvest index (HI) approach, assuming yield is a fraction (the HI) of the total above-ground biomass. Such models can be readily applied to several plant types by deriving realistic plant parameters such as radiation use efficiency (RUE), maturity type, leaf angle through the light extinction coefficient, and efficiency in partitioning the biomass through the HI.

In this paper, we describe various aspects of plant modelling that address different user goals. First, we describe some unique aspects of the generic plant model ALMANAC (Agricultural Land Management Alternatives with Numerical Assessment Criteria, Kiniry *et al.*, 1992). The model uses many of the same basic parameters to simulate plant growth as the current SWAT model, but ALMANAC is unique in its ability to accurately simulate competition for light, nutrients, and water for several plant species. We provide a description of the methodology to develop parameters for vegetation simulations by such process-based models as ALMANAC. Next, we describe how ALMANAC was adapted to simulate the diversity of species involved in forest succession after disturbance such as tree harvest or fire. We discuss differences between forestry and agricultural applications and describe how the revised ALMANAC model simulates complex successional changes in forest ecosystems. Finally, we discuss alternative physiological and physical process simulation techniques for light interception, nutrient partitioning and water uptake that could improve plant simulation. Our objectives are to provide an overview of new adaptations to vegetation models that could allow model users to simulate new hydrological problems, specifically intercropping and forest management, and to identify specific physiological process that can be improved in present models. This overview provides some possible future directions for vegetation simulation in hydrological models such as SWAT.

General summary of ALMANAC's plant model

The ALMANAC model simulates processes of plant growth and soil water balance, including light interception by leaves, dry matter production, and partitioning of biomass into grain. For crops, the model simulates a grain yield based on HI, which is grain yield as a fraction of total aboveground dry matter at maturity. ALMANAC simulates LAI, light interception with Beer's law, and potential daily biomass increase with a species-specific value of RUE. It can simulate weed impacts on crop yields and intercropping using a reasonable and easily implemented light competition model. Light intercepted by each species is a function of its extinction coefficient, its contribution to total leaf area, and its current height.

ALMANAC includes a generic LAI function. The development of LAI as a function of fraction of seasonal degree day sum follows an "s" curve, with two input parameters defining the curve. Daily increments of LAI growth can be reduced by water stress.

The ALMANAC model simulates the water balance, the nutrient balance, and the interception of solar radiation for one or more plant species. The model includes subroutines and functions related to the water balance, nutrient balances, and soil erosion from the EPIC model (Williams *et al.*, 1984) and adds details for plant growth.

The model has been extensively validated for row crops in a wide range of locations, drought conditions, and plant species. ALMANAC simulated mean crop yields in nine states in the USA with diverse soils and climate (Kiniry *et al.*, 1997), and at sites within Texas (Kiniry & Bockholt, 1998). When applied to maize (*Zea mays* L.) at 11 sites and sorghum (*Sorghum bicolor* (L.) Moench) at eight sites in Texas for the dry conditions of 1998, ALMANAC realistically estimated grain yields (Yun *et al.*, 2001). ALMANAC was used to simulate grasses, both in monoculture and with multiple species growing together. Kiniry *et al.* (1996, 2005) and McLaughlin *et al.* (2006) simulated Alamo switchgrass (*Panicum virgatum* L.) at diverse sites in the USA. In addition, ALMANAC was used to simulate range yields for a diverse set of ecological sites with two or more grass species competing, representing extremes of productivity for Texas (Kiniry *et al.*, 2002, 2007).

The model has been successfully applied in other situations to simulate two or more plant species competing. In the original paper (Kiniry *et al.*, 1992), ALMANAC estimated the impact of weed infestations on crop yields with several data sets from the literature. In addition, it accurately simulated spring wheat (*Triticum aestivum* L.) yields with different densities of competing oats (*Avena sativa* L.), oilseed rape (*Brassica napus* L.), and vetch (*Vicia sativa* L.) in France (Debaeke *et al.*, 1997).

Plant parameters for this model can be readily derived and validated using standardized procedures. Interception of light by the leaf canopy should be determined by measuring photosynthetically active radiation (PAR) interception during the season with a sensor such as the 0.8-m-long Sunfleck Ceptometer (Decagon, Pullman, Washington 99163, USA). Likewise, RUE is expressed in units of g of biomass per MJ of intercepted PAR. Constancy in using PAR for light interception measurement, calculation of light extinction coefficient (*k*) for Beer's law (as defined below), and RUE calculation is vital. As discussed by Kiniry (1999), incident total solar radiation is easily converted to PAR above the plant canopy by multiplying by a factor of 0.45 (Monteith, 1965; Meek *et al.*, 1984). Recently, Lizaso *et al.* (2003) reported a similar conversion factor of 0.43. PAR is the definitive band of wavelengths pertinent to photosynthetic responses inherent in the RUE approach. Differences in light interception between PAR and total solar radiation (as discussed by Jovanovic & Annandale, 1998; Kiniry, 1999) are avoided by making the total solar radiation to PAR conversion for the incident light above the plant canopy, before interception by leaves.

The *k* coefficient (Monsi & Saeki, 1953) is calculated from the fraction of PAR intercepted (FIPAR) and the LAI. Values for *k* are calculated for each harvest date of each cultivar as:

$$k = [\ln (1 - \text{FIPAR})]/\text{LAI} \qquad (1)$$

These measurements provide useful input values for LAI, *k* and RUE.

The Adapted ALMANAC model, ALMANAC$_{BF}$: forestry applications

The SWAT model is well adapted to simulations of forest management actions because it can easily handle long-term multi-scale simulations, it simulates water quantity and water quality, and the land-use approach of delineating hydrological response units on the landscape works well with foresters' land bases that use the forest stand as a distinct land unit (Putz *et al.*, 2003; Arnold & Fohrer, 2005). However, the forest growth module of SWAT requires major modifications to simulate the key processes of forest hydrology that are impacted by forest management practices.

Landscape units of forested watersheds are delineated as "forest stands" that consist of distinct areas of forest of a single or consistent combination of tree species of similar age and productivity. Unlike agriculture, the differences among sites as to how they will react to forest management (harvest and regrowth) are largely associated with site characteristics, not management decisions.

To simulate forest disturbance and regrowth, we model a forest stand existing on a specific ecosite Ecosite classification defines a site by its hydrological state (xeric to hydric) and nutrient richness (poor to very rich) (Beckingham & Archibald, 1996). The vegetation on the site will grow through a series of successional stages before returning to the mature forest state.

Existing forest growth models simulate forest management practices and environmental influences on stand growth and ecosystem function over long time periods (Running & Coughlin, 1988; Kimmins *et al.*, 1999; Peng *et al.*, 2002; Seely *et al.*, 2002; Welham *et al.*, 2002). These are generally complex and data intensive models that are difficult to adapt to catchment-scale modelling. Simple growth and yield models exist (Landsberg & Waring, 1997) but only for simulating pure (single species) even-aged canopies. As an alternative, the ALMANAC model was adapted to simulate the regrowth of vegetation on forested sites on the Boreal Plain after forest disturbance (MacDonald *et al.*, 2005; MacDonald *et al.*, 2008). The revised boreal forest version of the model (ALMANAC$_{BF}$) is conceptually similar to other simple forest growth models and forest modules (Landsberg & Waring, 1997; Peng *et al.*, 2002; Wattenbach *et al.*, 2005), but has the added advantage of simulating multiple species. We have developed the ALMANAC$_{BF}$ model to be integrated into SWAT as a forest disturbance and regrowth module. With the multi-species algorithms existing in the model, it can simulate the successional changes in forest regrowth after disturbance.

The largest impact on water quantity and quality in forests occurs in the first 10 years after disturbance due to tree harvesting (Burke *et al.*, 2005; Prepas *et al.*, 2006). For this reason, development of ALMANAC$_{BF}$ algorithms focused on simulations of the successional changes in vegetation in these initial stages after disturbance. The model also simulates the potential variability in forest growth trajectories in immature forests 10–50 years after disturbance. This approach addresses a gap in forest models that ignore the early years of stand establishment, focusing only on simulating young stand dynamics after forest canopies have closed.

Study region: forests of the Boreal Plain

The Boreal Plain formed on deep rich soils of the northern Great Plains of North America. Stands vary in their moisture regime (xeric to hygric) and site richness (poor to rich). Gradients are observed in the speed and amount of competitive vegetation (grasses, forbs and woody shrubs) that establish on a site after disturbance. Invasive vegetative biomass in the years immediately following harvest in xeric poor sites and mesic medium sites will range from 250 to 1000 kg ha^{-1} year^{-1}. In rich sub-hygric and hygric sites, biomass production ranges from 3000 to 8000 kg ha^{-1} year^{-1}.

The mature forests that develop on the Boreal Plain consist of a variety of species combinations. Mature upland forests consist of lodgepole pine (*Pinus contorta* Douglas ex Loudon) and trembling aspen (*Populus tremuloides* Michx). Richer moist sites have white spruce (*Picea glauca* (Moenh) Voss) and deciduous stands—trembling aspen/balsam poplar (*Populus balsamifera* L.). Wetlands and sites with organic soils are predominantly slow growing pure black spruce (*Picea mariana* (Mill.), Britton *et al.*) and mixed black spruce/deciduous stands (Beckingham & Archibald, 1996; Smith *et al.*, 2003). Forest stands often consist of complex mixed forest canopies. A catchment-scale growth model must capture the important forest dynamics without spending excessive simulation time on the complexities of forest growth.

The ALMANAC$_{BF}$ was created to simulate this range of variability in vegetation. In other work we carried out a series of theoretical model simulations using parameters representing the range of forest stands that occur on the Boreal Plain (MacDonald *et al.*, 2005; MacDonald *et al.*, 2008). We demonstrated how the model simulates the successional changes in different forest stands in the first 50 years after disturbance with respect to biomass, light interception, and leaf area index. The simulations use data taken from weather stations established in the FORWARD (Forest Watershed and Riparian Disturbance) research area of northern Alberta in Canada (Smith *et al.*, 2003; Prepas *et al.*, 2006), and soil information from the Agricultural Region of Alberta Soil Inventory Database (Knapik & Lindsay, 1983).

The ALMANAC$_{BF}$ algorithm function and application

The Canadian forest industry uses geographically referenced databases developed from aerial photo interpretation to define the characteristics of individual stands across the boreal forest. ALMANAC$_{BF}$ input files were created from forestry databases that described the species that make up a given stand (strata), an indication of tree productivity (site productivity class, related to stem number per hectare) and an indicator of the intensity of competitive vegetation (ecosite) in the initial years after disturbance. Immediately after disturbance, forest sites are invaded by annual plants, followed by perennial shrubs and, over time, evolve into mature deciduous/coniferous tree canopies. The strata, site productivity class and ecosite will determine the speed and productivity of vegetation establishment. From this information the growth trajectory of an individual landscape unit can be defined.
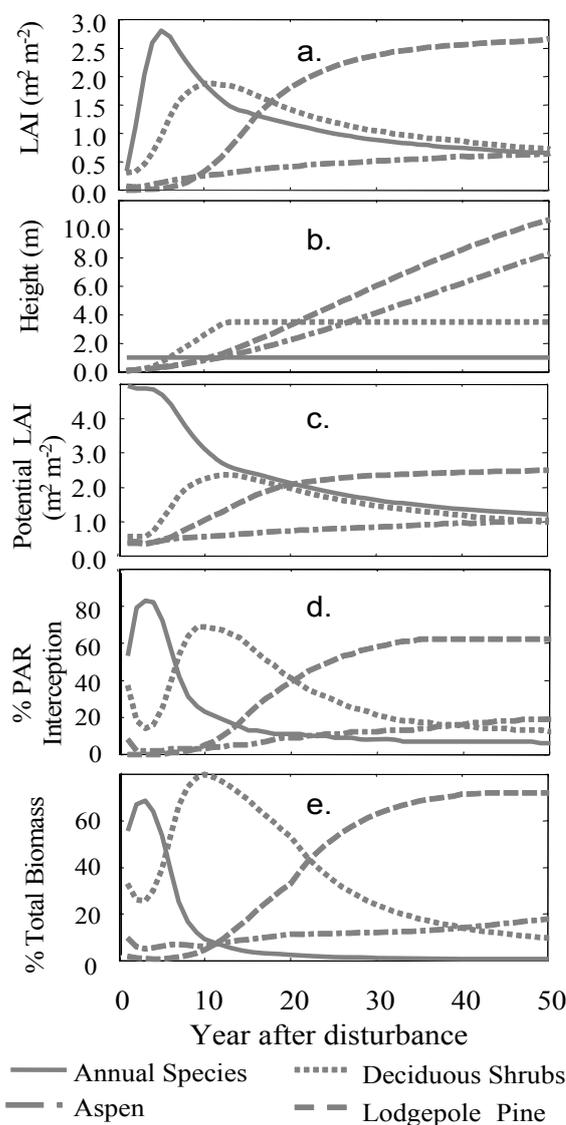

Fig. 1 Transformations in simulated vegetation parameters over the initial 60 years after disturbance in a mixed lodgepole pine/trembling aspen stand for four species growing simultaneously, an annual grass, a tall shrub, and two tree species: (a) actual LAI, limited by water and temperature stress; (b) canopy height; (c) potential LAI, maximum at complete establishment without growth limitations; (d) PAR interception, modified by LAI occupancy and height; and (e) percentage of standing biomass. Initial percentage cover values were 50% lodgepole pine, 50% trembling aspen (adapted from MacDonald *et al.*, 2008).

For tree species, ALMANAC$_{BF}$ uses the RUE to calculate biomass, but uses species specific allometric equations (Ter-Mikaelian & Korzukhim, 1997) and self thinning equations (changes in stem number of the forest stand over time) to partition biomass into different woody and foliar biomass (MacDonald *et al.*, 2005, 2008). Leaf area index is proportional to foliar biomass, which is a function of stem number. Consequently, stand productivity is proportional to stem density. Dense forest stands have smaller trees, with a lower ratio of foliar biomass to stem biomass (and lower LAI). The model uses sigmoid curves ("s curves") based on growth degree-day to describe annual growth (deciduous bud burst and conifer flush). Likewise, to simulate the gradual establishment of species on a site over time, sigmoid equations are used to describe long-term height and leaf area growth, using year as the dependent variable as opposed to heat units.

After disturbance, pioneer species can take several years to establish on a site. Simulations of two types of conifer-dominated boreal mixed wood sites demonstrate how the multi-species
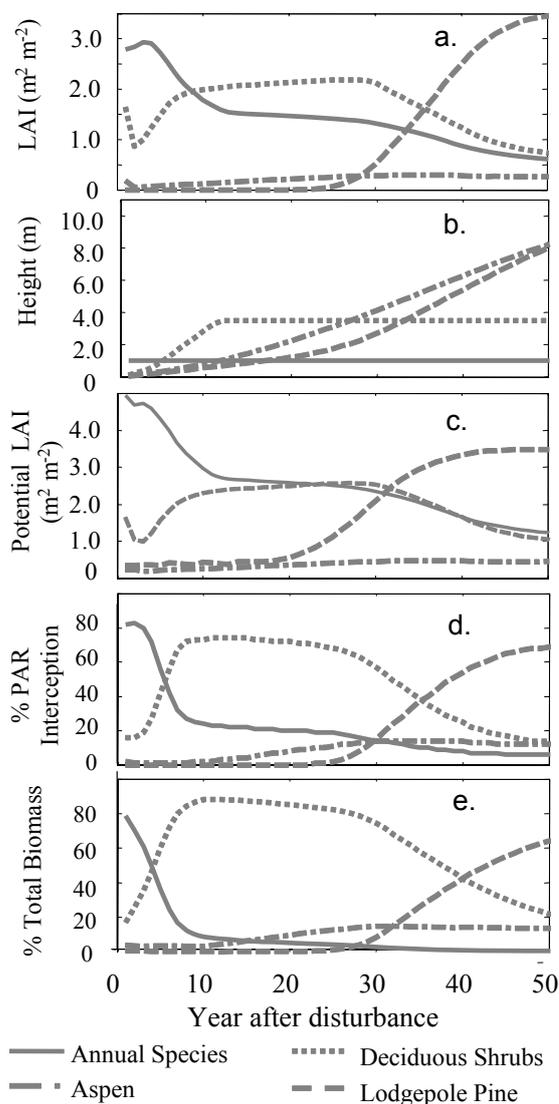

Fig. 2 Transformations in simulated vegetation parameters over the initial 60 years after disturbance in a mixed white spruce/trembling aspen stand for four species growing simultaneously, an annual grass, a tall shrub, and two tree species: (a) actual LAI, limited by water and temperature stress; (b) canopy height; (c) potential LAI, maximum at complete establishment without growth limitations; (d) PAR interception, modified by LAI occupancy and height; and (e) percentage of standing biomass. Initial percentage cover values were 65% white spruce, 35% trembling aspen (adapted from MacDonald *et al.*, 2008).

algorithms simulate the successional process (Figs 1 and 2). The key element in the multi-species growth simulations is the interaction of the relatively simple light partitioning equations with the long-term leaf area development equations and a simple algorithm that limits potential leaf area based on species height and leaf area index in previous years. Leaf area for each species regrowing on a forested site after disturbance follows a sigmoid equation that has species-specific parameters (Figs 1(a) and 2(a)). Rapidly growing species (annuals and perennial shrubs) will achieve their maximum leaf area in 5–10 years. As one species begins to grow taller than other species (Figs 1(b) and 2(b)), the potential leaf area is reduced proportionally to the species height and occupancy in the total canopy. For example, annual species in the first two years after disturbance establish on sites essentially without restriction. However, as they begin to be shaded by the perennial shrub canopy their potential leaf area is restricted by more than 50%. As the tree canopy becomes established, potential leaf area is once again restricted by 50% (Figs 1(c) and 2(c)). The algorithms limiting LAI for understory plants simulate the reduced area that plants are able to exploit to achieve growth due to both light and physical constraints.

While the algorithms describing LAI establishment and limitations describe the physical changes in the presence of different species on the site over time, the ALMANAC light partitioning equations divide PAR among the different species based on species height and relative occupancy in the canopy. PAR interception of annual species is reduced from 85% to 6% over the first 35 years after stand establishment (Figs 1(d) and 2(d)). Likewise, the biomass of annual species becomes an insignificant portion of total standing biomass on the site at 30 years.

Crop trees such as trembling aspen and lodgepole pine may become established rapidly, whereas species such as white spruce may take several years (Figs 1 and 2). The simulated successional process of white spruce stands left to natural regeneration begins with a rapid development of annual and shrub species in year 1 (LAI = 4.5) followed by perennial shrubs mixed with aspen beginning to dominate the canopy in years 8–10. White spruce begins to play a significant role in LAI only in years 25–40. In contrast, the successional process of simulated lodgepole pine stands has a slow development of annual species (LAI = 0.6) in year 1 after disturbance and the site is dominated by lodgepole pine by year 20.

Differences in the dominant vegetation on a site will influence annual evapotranspiration patterns by influencing the timing of peaks in transpiration (Bosch & Hewlett, 1982), canopy interception (Aussenac & Boulangeat, 1980; Wattenbach *et al.*, 2005), soil warming (Bonan 1991; Chen *et al.*, 1999), and nutrient uptake and cycling (Prescott, 2002). Residue deposited by deciduous and annual species have different nutrient concentrations than coniferous species. Consequently, decomposition rates and nutrient release vary with successional changes in the forest canopy (Gower *et al.*, 2000; Prescott *et al.*, 2000; Hagen-Thorn *et al.*, 2004).

The choice of ALMANAC to simulate forest growth on the Canadian Boreal Plain was due first of all to its compatibility with the plant growth processes in the current SWAT plant growth model. Also, it uses a daily time step and simulates the growth of mixed canopies, an essential feature of the mixed forests of the Boreal Plain. Models that simulate the simultaneous growth of multiple species tend to be complex and not necessarily suited to catchment-scale simulations (Botkin *et al.*, 1972; Kimmins *et al.*, 1999; Bartelink, 2000). ALMANAC uses the same soil and weather information as SWAT. The soil parameters are compatible with Canadian and US Government soil survey databases.

Advances in application of physical principles in vegetation modelling

It is important to balance assumptions, inputs, and model structure complexity when building simulation models. Processes operating in soil-crop models are intimately related, yet these links are not always explicitly recognized. A typical case is considering the interception of PAR radiation by crop canopies independently of the overall solar radiation balance.

The SWAT and EPIC models simulate light (PAR) interception, assuming a constant value for light extinction coefficient (k) of 0.6 for PAR. The ALMANAC model uses different values of k for different species and for different row spacings. Since photosynthesis is driven by PAR, these

models calculate PAR interception in order to simulate growth based on RUE. PAR can be estimated as 45% of total solar radiation, as discussed above. However, only 2% or less of the energy in PAR wavebands is used in photosynthesis. The remainder of the energy in the PAR waveband and the energy in the ultraviolet and near-infrared radiation is dissipated as sensible or latent heat, or stored heating the soil, leaves, stems, and tree trunks. A method to deal with radiation, so that intercepted PAR calculations to compute crop growth are consistent with those used to compute the energy balance components can be used to calculate interception of short wave radiation by a leaf canopy. A function for estimating the extinction coefficient for PAR (k_{PAR}) from the extinction coefficient for total solar radiation (k_s) is:

$$k_{PAR} = 1.62k_s^{1.16} \tag{2}$$

For example, if $k_s = 0.43$ then $k_{PAR} = 0.61$, so $k_{PAR}: k_s = 1.42$. A similar ratio of 1.34 for $k_{PAR}: k_s$ was reported by Monteith & Unsworth (1990).

Campbell (1985) indicated that partitioning soil evaporation and transpiration (and evaporation from plant residues standing or flat on the soil surface) can be estimated using the fraction of the solar radiation intercepted by each component. This method partitions transpiration from evaporation in field-measured water use of spring barley (*Hordeum vulgare* L.) (Kemanian *et al.*, 2005). SWAT simulates soil evaporation using the LAI (Ritchie, 1972). When LAI is equal to or greater than 3, all ET is allocated to transpiration. The fraction allocated to soil evaporation increases linearly as LAI decreases from 3.0 to 0.0. Thus, for a moist soil surface and for a crop reaching a LAI of 5.8, the estimated fractional evaporation increases and then has a plateau (Fig. 3).

We compared the two methods by assuming $k_s = 0.43$ ($k_{PAR} = 0.61$) and found that soil evaporation predicted with either method was similar for LAI < 1.5, but was greater when LAI > 1.5 for the total solar radiation-based method (Fig. 3). The solar radiation based method could improve the simulation of soil surface water content, having a major impact on simulated runoff volumes. Efforts at improving radiation interception simulation (and measurement) should concentrate on early growth (LAI < 1) for two reasons: first, the assumption of randomness in leaf distribution implicit in using the extinction coefficient approach is clearly violated in row crops at
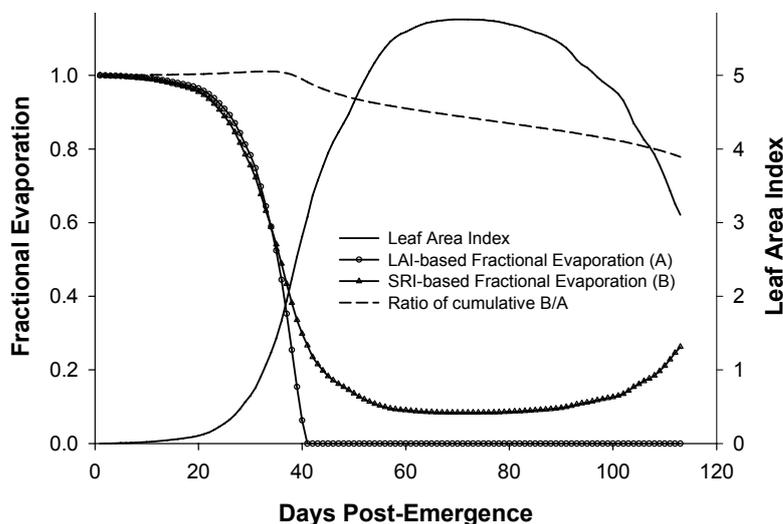

Fig. 3 Hypothetical partitioning of total evapotranspiration to soil evaporation for a soil that is continuously moist (soil moisture does not limit evaporation rate) and not covered by residues. The leaf area index evolution represents a hypothetical annual crop with a cycle from seedling emergence to maturity of 113 days. The LAI-based fractional evaporation is based on Ritchie (1972) as used in SWAT. The SRI-based approach (Solar Radiation Interception) is based on the fractional transmitted solar radiation with extinction coefficient of solar radiation = 0.43. The ratio of cumulative fractional evaporation indicates that if the evaporation demand were the same during the entire growing cycle. The LAI-based method would predict a total evaporation approximately 23% lower than the solar radiation interception-based method.

low LAI when there is minimum overlap among leaves, and second, because changes in canopy cover affect soil evaporation the most at low LAI.

Root function: water uptake

Root growth, turnover, and deposition have been reviewed in detail recently by Amos & Walters (2006) for maize and by Bolinder *et al.* (2007) for several crops and perennials. We briefly focus here on root function, particularly water uptake. Water uptake can be simulated based on the balance between transpirational demand, which is a function of atmospheric and canopy conditions, and the potential supply by the soil–plant system. When soil water content is relatively high ($\psi_s \sim 0$ J kg^{-1} water potential) the limitation to water flow is mostly determined by resistance in the plants. The two most important sources of resistance are the endodermis and the stomata. When the soil water supply is below that demanded by the atmosphere, the stomata close, increasing the resistance to water flow and thus preventing dehydration. Regulation of stomata closure is complex, but nonetheless responds from the hydrodynamic point of view to soil water potential. Roots "sense" dry or drying soils through an undefined mechanism, with communication from roots to leaves through hormonal signals (Tardieu *et al.*, 1991). Resistance to water flow increases in the xylem due to cavitation (Sperry *et al.*, 1998) and local (leaf) dehydration (Mott & Parkhurst, 1991). These effects can be reasonably simulated by a single function of stomatal conductance response to leaf water potential (Choudhury & Idso, 1985; Fig. 4). However, the link between leaf water potential and stomatal conductance is likely not direct. Stomatal conductance also responds to photosynthesis (Cowan, 1977). These linkages are considered in coupled photosynthesis–transpiration models, but such complex modelling approaches are not practical for comprehensive hydrological models.

There are several literature reviews on modelling approaches to simulate water and nutrient uptake. In a recent review, Wang & Smith (2004) described empirical approaches. These use a mixture of common sense and mathematical functions to represent the dependence of soil water uptake on root density, soil water content, and root distribution. There are also analytical approaches that consider water potential as the driving force for water movement in the soil–plant continuum. A physically-based approach for modelling water uptake was developed by Campbell (1991) and applied by Jara & Stöckle (1999) and Stöckle *et al.* (2003). Some considerations of this approach that are potentially useful in SWAT include: (a) impact of soil structure as well as other factors on root distribution and therefore on soil resistance, particularly at low root length density; (b) more accurate values for root resistance and leaf resistance to water flow, calculated from
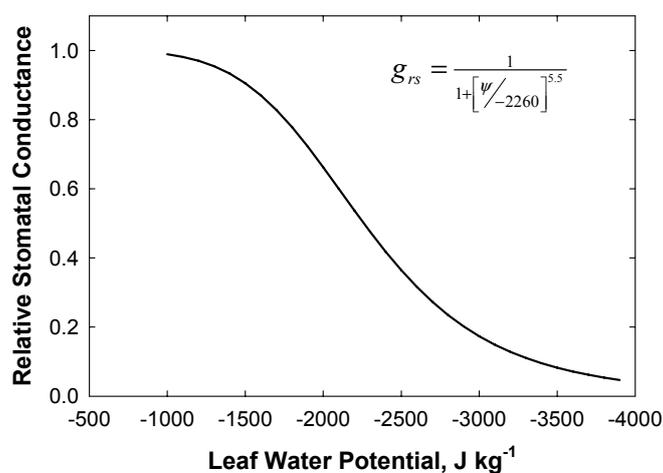

$$g_{rs} = \frac{1}{1+\left[\psi\Big/{-2260}\right]^{5.5}}$$

Fig. 4 Relative response of the stomatal conductance to leaf water potential as reported by Choudhury & Idso (1985) for the wheat cultivar Anza. The value of the power (5.5 in the figure) ranges from 5 to 10, and 7 seems to fit several crops. The reference leaf water potential (ψ) (2260 in the figure) ranges from -1200 to -2400 J kg^{-1}.

measurements; and (c) the leaf resistance should be allowed to vary with water stress, as cavitation of the water columns in the xylem causes an increase in the plant hydraulic resistance (Stiller *et al.*, 2003). In the model, it was assumed that the roots are homogeneously distributed i.e. r_s, the radius of the soil cylinder around a linear root segment is $r_s = (\pi l)^{-1/2}$ where l is the root length density (m m^{-3}). If the soil distribution is not uniform, an "effective" l needs to be computed, preferably linked to measurable soil properties and plant genotype characteristics.

Nutrients partitioning in simple models: nitrogen

Intensive management of agroecosystems has changed the flow of nutrients at field and watershed levels. Agricultural lands receive inputs of nutrients in the form of fertilizer and nitrogen fixing legumes. Nutrients leave fields in harvested grain, harvested hay, percolating water and runoff water, as well as in sediments and organic matter lost to erosion. Thus, correctly simulating the balance of nutrients on a point basis for a crop has relevant implications at the landscape level. Taking nitrogen as an example, we discuss in this section a simple approach for simulating the nitrogen balance of annual grain crops. Simulating grain (N_g) and straw (N_s) nitrogen concentration is important in short-term and long-term simulations by agricultural models to accurately estimate nitrogen removal from the soil when grain is harvested. In addition, the residue or straw nitrogen concentration affects the speed of residue decomposition, the carbon balance, the degree of immobilization of mineral nitrogen, and denitrification. Small errors in the nitrogen balance can have major impacts on the C:N ratio of the residue. For example, wheat yields of 4 Mg ha^{-1} will leave approximately 6 Mg ha^{-1} of above-ground residue. Residue with a N_s of 4 g N kg^{-1} dry matter (24 kg N ha^{-1}) has a C:N ratio of approx. 100. A modest increase in the nitrogen left in the straw of 15 kg N ha^{-1} will lower the C:N ratio to 66. These minor variations in nitrogen concentration have a major impact on residue decomposition.

Simulation models like EPIC, ALMANAC, and SWAT simulate the aboveground plant nitrogen and phosphorus concentrations throughout the season based on optimal plant concentrations (which vary from seedling emergence to maturity) and the available N and P in the rooting zone of the soil. Aboveground N and P are allocated to grain and straw at harvest as:

$$N_g = N_{gr}(N_t/N_{br})^{0.1} \tag{3}$$

where N_g is the grain nitrogen concentration at harvest, N_{gr} is a reference grain nitrogen concentration, N_t is the aboveground nitrogen concentration at harvest, and N_{br} is a reference N_t. Both N_{gr} and N_{br} are input parameters. The actual harvest index does not affect the computation of nitrogen concentration of grain and straw.

Kemanian *et al.* (2007) proposed a simple approach to partition nitrogen between grain and straw at harvest. The only inputs required are N_t and HI. The model has five parameters for each crop, four of which are easily obtained from the literature and one needs calibration. Parameters were developed for wheat, barley, sorghum and maize. At a typical aboveground nitrogen concentration of wheat at maturity of 10 g kg^{-1}, the grain nitrogen concentration can vary from 20 (HI = 0.45) to 30 g kg^{-1} (HI = 0.25) (Fig. 5). Under these conditions, the NHI ranged from 0.65 to 0.85. The method currently in EPIC, also included for comparison, is less sensitive to HI and N_t. Improved results are obtained with the EPIC method if the power 0.1 is replaced by 0.8, but the sensitivity to HI is not captured. Including approaches based on simple physiological principles could improve the nitrogen balance of comprehensive hydrological models. The possibility of extending this approach to other crops and nutrients needs to be explored.

SUMMARY

In this paper, we presented some approaches for modelling plants applicable to hydrological models like SWAT, in the hope of improving the accuracy in simulating the water and nutrient biogeochemical cycles. We described the generic plant model ALMANAC and demonstrated how a revised version of the ALMANAC model simulated complex successional changes in forest
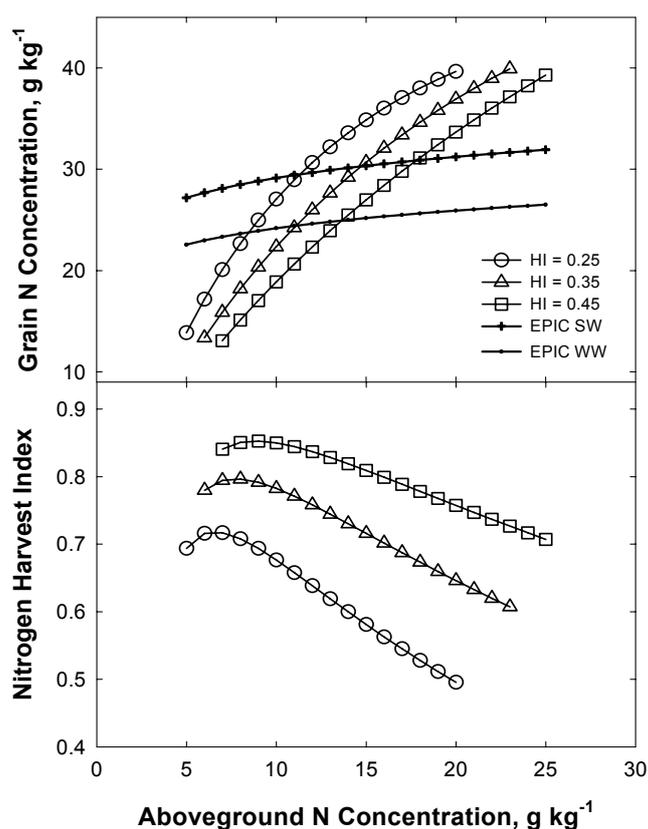
Fig. 5 Variation in wheat grain nitrogen concentration and nitrogen harvest index as a function of the aboveground nitrogen concentration and harvest index. The graphs were generated with the model and parameters presented by Kemanian *et al.* (2007). The approach used in EPIC is explained in the text.

ecosystems. In the final three sections, we discussed alternative physiological and physical process simulation techniques that can increase simulation accuracy in SWAT-type models.

REFERENCES

Amos, B. & Walters, D. T. (2006) Maize root biomass and net rhizodeposited carbon: an analysis of the literature. *Soil Sci. Soc. Am. J.* **70**, 1489–1503.

Arnold, J. G., Srinivasan, R., Muttiah, R. S. & Williams, J. R. (1998) Large area hydrologic modelling and assessment, Part I. Model development. *J. Am. Water Resour. Assoc.* **34**, 73–89.

Arnold, J. G. & Fohrer, N. (2005) SWAT2000: current capabilities and research opportunities in applied watershed modelling. *Hydrol. Processes* **19**, 563–572.

Aussenac, G. & Boulangeat, C. (1980) Rainfall interception and actual evapotranspiration in broadleaved (*Fagus sylvatica*) and coniferous (*Pseudotsuga mensiesii*) stands. *Ann. Sci. Forest.* **37**, 91–107.

Bartelink, H. H. (2000) A growth model for mixed forest stands. *For. Ecol. Manage.* **134**, 29–43.

Beckingham J. D. & Archibald, J. H. (1996) Field guide to ecosites of northern Alberta. Special Report 5, Canadian Forest Service.

Bolinder, M. A., Janzen, H. H., Gregorich, E. G., Angers, D. A. & VandenBygaart, A. J. (2007) An approach for estimating net primary productivity and annual carbon inputs to soil for common agricultural crops in Canada. *Agric, Ecosyst. Environ.* **118**, 29–42.

Bonan, G. B. (1991) A biophysical surface energy budget analysis of soil temperature in the Boreal Forests of interior Alaska. *Water Resour. Res.* **27**, 767–781.

Bosch, J. M. & Hewlett, J. D. (1982) A review of catchment experiments to determine the effect of vegetation changes on water yield and evapotranspiration. *J. Hydrol.* **55**, 3–23.

Botkin, D. B., Janak, J. F. & Wallis, J. R. (1972) Some ecological consequences of a computer model of forest growth. *J. Ecol.* **60,** 849–872.

Burke, J. M., Prepas, E. & Pinder, S. (2005) Runoff and phosphorus export patterns in large forested watersheds on the western Canadian Boreal Plain before and for 4 years after wildfire. *J. Environ. Engng Sci.* **4**, 319–325.

Campbell, G. S. (1985) *Solar Physics with BASIC*: *Transport Models for Soil–Plant Systems*. Elsevier, Amsterdam.

Campbell, G. S. (1991) Simulation of water uptake by plants roots. In: *Modelling plant and soil systems* (ed. by J. Hanks & J. T. Ritchie). *Am. Soc. Agron. Mono.* **31**, 273–285.

Chen, J., Saunders, S. C., Crow, T. R., Naiman, R. J., Brosofske, K. D., Mroz, G. D., Brookshire, B. L. & Franklin, J. F. (1999) Microclimate in forest ecosystem and landscape ecology. *BioScience* **49**, 288–297.

Choudhury, B. J. & Idso, S. B. (1985) Evaluating plant canopy resistance of field-grown wheat from concurrent diurnal observations of leaf water potential, stomatal resistance, canopy temperature, and evapotranspiration flux. *Agric. For. Met.* **34**, 67–76.

Cowan, I. R. (1977) Stomatal behaviour and environment. *Adv. Bot. Res.* **4**, 117–228.

Debaeke, P., Caussanel, J. P., Kiniry, J. R., Kafiz, B. & Mondragon, G. (1997) Modelling crop-weed interactions in wheat with ALMANAC. *Weed Res.* **37**, 325–341.

Gower, S. T., Hunter, A., Campbell, J., Vogel, J., Veldhuis, H., Harden, J., Trumbore, S., Norman, J. M. & Kucharik, C. J. (2000) Nutrient dynamics of the southern and northern BOREAS boreal forests. *Ecoscience* **7**, 481–490.

Hagen-Thorn, A., Armolaitis, K., Callesen, I. & Stjernquist, I. (2004) Macronutrients in tree stems and foliage: a comparative study of six temperate forest species planted at the same sites. *Ann. For. Sci.* **61**, 489–498.

Jara, J. & Stöckle, C. O. (1999) Simulation of water uptake in maize, using different levels of process detail. *Agron. J.* **91**, 256–265.

Jovanovic, N. & Annandale, J. G. (1998) Measurement of radiant interception of crop canopies with the LAI-2000 plant canopy analyzer. *S. Afr. Tydskr. Plant Grond* **15**, 6–13.

Kemanian, A. R., Stöckle, C. O. & Huggins, D. R. (2005) Barley transpiration-use efficiency. *Agric. For. Met.* **130**, 1–11.

Kemanian, A. R., Stöckle, C. O. & Huggins, D. R. (2007) Estimating grain and straw nitrogen concentration in grain crops based on aboveground nitrogen concentration and harvest index. *Agron. J.* **99**, 158–167.

Kimmins, J. P., Mailly, D. & Seely, B. (1999) Modelling forest ecosystem net primary production: the hybrid simulation approach used in FORECAST. *Ecol. Model.* **122**, 195–224.

Kiniry, J. R. (1999) Response to questions by Sinclair and Muchow. *Field Crops Res.* **62**, 245–247.

Kiniry, J. R. & Bockholt, A. J. (1998) Maize and sorghum simulation in diverse Texas environments. *Agron. J.* **90**, 682–687.

Kiniry, J. R., Williams, J. R., Gassman, P. W. & Debaeke, P. (1992) A general process-oriented model for two competing plant species. *Trans. Am. Soc. Agric. Engrs* **35**, 801–810.

Kiniry, J. R., Sanderson, M. A., Williams, J. R., Tischler, C. R., Hussey, M. A., Ocumpaugh, W. R., Read, J. C., VanEsbroeck, G. & Reed, R. L. (1996) Simulating Alamo switchgrass with the ALMANAC model. *Agron J.* **88**, 602–606.

Kiniry, J. R., Williams, J. R., Vanderlip, R. L., Atwood, J. D., Reicosky, D. C., Mulliken, J., Cox, W. J., Mascagni, H. J. Jr, Hollinger, S. E. & Wiebold, W. J. (1997) Evaluation of two maize models for nine U.S. locations. *Agron. J.* **89**, 421–426.

Kiniry, J. R., Sanchez, H., Greenwade, J., Seidensticker, E., Bell, J. R., Pringle, F., Peacock, G. Jr & Rives, J. (2002) Simulating grass productivity on diverse range sites in Texas. *J. Soil & Water Conserv.* **57**, 144–150.

Kiniry, J. R., Cassida, K. A., Hussey, M. A., Muir, J. P., Ocumpaugh W. R., Read, J. C., Reed, R. L., Sanderson, M. A., Venuto, B. C. & Williams, J. R. (2005) Switchgrass simulation by the ALMANAC model at diverse sites in the southern US. *Biomass & Bioenergy* **29**, 419–425.

Kiniry, J. R., Burson, B. L., Evers, G. W., Williams, J. R., Sanchez, H., Wade, C., Featherston, J. W. & Greenwade, J. (2007) Coastal bermudagrass, bahiagrass, and native range simulation at diverse sites in Texas. *Agron. J.* **99**, 450–461.

Knapik, L. J. & Lindsay, J. D. (1983) Reconnaissance soil survey of the Iosequn Lake Area, Alberta. Report no. 43, Alberta Research Council, Edmonton, Alberta, Canada.

Landsberg, J. J. & Waring, R. H. (1997) A generalised model of forest productivity using simplified concepts of radiation use efficiency, carbon balance and partitioning. *For. Ecol. Manage.* **95**, 209–228.

Lizaso, J. I., Batchelor, W. D., Westgate, M. E. & Escharte, L. (2003) Enhancing the ability of CERES-Maize to compute light capture. *Agric. Systems* **76**, 293–311.

MacDonald, J. D., Kiniry, J., Arnold, J., McKeown, R., Whitson, I., Putz, G. & Prepas, E. E. (2005) Developing parameters to simulate trees with SWAT. In: *Proc. Third Int. SWAT 2000 Conf.* (Zurich, Switzerland, 11–15 July 2005) (ed. by K. Abbaspour & R. Srinivasan). Texas Water Resources Institute, College Station, Texas, USA.

MacDonald, J. D., Kiniry, J., Arnold, J., McKeown, R., Whitson, I., Putz, G. & Prepas, E. E. (2008) A multi-species, process based vegetation simulation model to estimate important variables in evapotranspiration after forest disturbance. *J. Environ. Eng. Sci.* (in press).

McLaughlin, S. B., Kiniry, J. R., Taliaferro, C. M. & Ugarte, D. D. (2006) Projecting yield and utilization potential of switchgrass as an energy crop. *Adv. Agron.* **90**, 267–297.

Meek, D. W., Hatfield, J. L., Howell, T. A., Idso, S. B. & Reginato, R. J. (1984) A generalized relationship between photosynthetically active radiation and solar radiation. *Agron. J.* **76**, 939–945.

Monsi, M. & Saeki, T. (1953) Über den Lichtfaktor in den Pflanzengesellschaften und seine Bedeutung fur die Stoffproduktion. *Japan J. Bot.* **14**, 22–52.

Monteith, J. L. (1965) Radiation and crops. *Experim. Agric.* **1**, 241–251.

Monteith, J. L. & Unsworth, M. H. (1990) *Principles of Environmental Physics*. Edward Arnold, London, UK.

Mott, K. A. & Parkhurst, D. F. (1991) Stomatal responses to humidity in air and helox. *Plant Cell Environ.* **14**, 509–515.

Peng, C., Liu, J., Dang, Q., Apps, M. J. & Hong, J. (2002) TRIPLEX: a generic hybrid model for predicting forest growth and carbon and nitrogen dynamics. *Ecol. Model.* **153,** 109–130.

Prepas, E. E., Burke, J. M., Whitson, I. R., Putz, G. & Smith, D. W. (2006) Associations between watershed characteristics, runoff, and stream water quality: hypothesis development for watershed disturbance experiments and modelling in the Forest Watershed and Riparian Disturbance (FORWARD) Project. *J. Environ. Engng Sci.* **5**, 27–37.

Prescott, C. E. (2002) The influence of the forest canopy on nutrient cycling. *Tree Physiol.* **22**, 1193–1200.

Prescott, C. E., Zabek, L. M., Staley, C. L. & Kabzems, R. (2000) Decomposition of broadleaf and needle litter in forests of British Columbia: influences of litter type, forest type, and litter mixtures. *Can. J. For. Res.* **30**, 1742–1750.

Putz, G., Burke, J. M., Smith, D. W., Chanasyk, D. S., Prepas, E. E. & Mapfuma, E. (2003) Modelling the effects of boreal forest landscape management upon streamflow and water quality: Basic concepts and considerations. *J. Environ. Engng Sci.* **2**, S87–S101.

Ritchie, J. T. (1972) Model for predicting evaporation from a row crop with incomplete cover. *Water Resour. Res.* **8**, 1204–1213.

Running, S. W. & Coughlin, J. C. (1988) General model of forest ecosystem processes for regional applications, hydrological balance, canopy gas exchange and primary production processes. *Ecol. Model.* **42**, 125–154.

Seely, B., Welham, C. & Kimmins, H. (2002) Carbon sequestration in a boreal forest ecosystem: results from the ecosystem simulation model, FORECAST. *For. Ecol. Manage.* **169**, 123–135.

Smith, D. W., Prepas, E. E., Putz, G., Burke, J. M., Meyer, W. L. & Whitson, I. (2003) The forest watershed and riparian disturbance study: a multi-disciplinary initiative to evaluate and manage watershed disturbance on the boreal plain of Canada. *J. Environ. Engng Sci.* **2**, S1–S13.

Sperry, J. S., Adler, F. R., Campbell, G. S. & Comstock, J. P. (1998) Limitation of plant water use by rhizosphere and xylem conductance: results from a model. *Plant, Cell & Environ.* **21**, 2347–2359.

Srinivasan, R., Arnold, J. G., Muttiah, R. S., Walker, C. & Dyke, P. T. (1993) Hydrologic Unit Model for the United States (HUMUS). In: *Proc. Advances in Hydro-Science and Engineering*, 451–456. University of Mississippi, Mississippi State, Mississippi, USA.

Stiller, V., Renee Lafitte, H. & Sperry, J. S. (2003) Hydraulic properties of rice and the response of gas exchange to water stress. *Plant Physiol.* **132**, 1698–1706.

Stöckle, C. O., Donatelli, M. & Nelson, R. (2003) CropSyst, a cropping system simulation model. *Europ. J. Agron.* **18**, 289–307.

Tardieu, F., Katerji, N., Bethenod, O., Zhange, J. & Davies, W. J. (1991) Maize stomatal conductance in the field, its relationship with soil and plant water potentials, mechanical constraints and ABA concentration in the xylem sap. *Plant Cell Environ.* **14**, 121–124.

Ter-Mikaelian, M. T. & Korzukhin, M. D. (1997) Biomass equations for sixty-five North American tree species. *For. Ecol. Manage.* **97**, 1–24.

Wang, E. & Smith, C. J. (2004) Modelling the growth and water uptake function of plant root systems: a review. *Austr. J. Agric. Res.* **55**, 501-523.

Wattenbach, M., Hattermann, F., Weng, R., Wchsung, F., Krysanova, V. & Badeck, F. (2005) A simplified approach to implement forest eco-hydrological properties in regional hydrological modelling. *Ecol. Model.* **187**, 40–59.

Welham, C., Seely B. & Kimmins, H. (2002) The utility of the two pass harvesting system: an analysis using the ecosystem simulation model FORECAST. *Can. J. For. Res.* **32**, 1071–1079.

Williams, J. R., Jones, C. A. & Dyke, P. T. (1984) A modelling approach to determining the relationship between erosion and soil productivity. *Trans. Am. Soc. Agric. Engrs* **27**, 129–144.

Williams, J. R., Dyke, P. T., Fuchs, W. W., Benson, V. W., Rice, O. W. & Taylor, E. D. (1990) *EPIC – Erosion/Productivity Impact Calculator: 2. User Manual*. (ed. by A. N. Sharpley & J. R. Williams). US Dept of Agric. Tech. Bulletin no. 1768.

Yun, X., Kiniry, J. R., Nedbalek, V. & Rosenthal, W. D. (2001) Maize and sorghum simulations with CERES-Maize, SORKAM, and ALMANAC under water-limiting conditions. *Agron. J.* **93**, 1148–1155.